

Effects of Divalent Cations on Voltage-Gated Ca^{2+} Channels and Depolarization-Induced $[\text{Ca}^{2+}]_i$ Transients of Freshly Isolated Pyramidal Cells of the Rat Dorsal Cochlear Nucleus

CS HARASZTOSI, Z RUSZNAK, L KOVACS AND G SZUCS

*Department of Physiology, University of Debrecen,
Medical and Health Science Centre, Medical School Hungary*

Abstract. The effects of divalent cations on voltage-activated Ca^{2+} channels and depolarization-evoked cytoplasmic $[\text{Ca}^{2+}]_i$ elevations were studied in pyramidal neurones isolated from the dorsal cochlear nucleus of the rat. Ca^{2+} currents were recorded using the whole cell configuration of the patch-clamp technique. $10 \mu\text{mol l}^{-1} \text{Cd}^{2+}$ exerted a greater blocking effect on the high-voltage activated (HVA) currents than on the low-voltage activated (LVA) ones (decrease to $26.6 \pm 2.5\%$ and to $87.8 \pm 2.1\%$, respectively). The blocking effect of $200 \mu\text{mol l}^{-1} \text{Cd}^{2+}$ was more pronounced and the difference between the effect on the HVA and LVA currents became smaller (decrease to $11.7 \pm 2.1\%$ and to $32.4 \pm 2.7\%$, respectively). $200 \mu\text{mol l}^{-1} \text{Ni}^{2+}$ reduced the LVA component more effectively (to $77.6 \pm 5.4\%$) than the HVA one (to $86.9 \pm 2.6\%$). Cytoplasmic $[\text{Ca}^{2+}]_i$ changes were measured applying a fluorimetric technique (Fura-2). $10 \mu\text{mol l}^{-1} \text{Cd}^{2+}$ decreased the peak values of $50 \text{mmol l}^{-1} \text{K}^+$ depolarization-induced $[\text{Ca}^{2+}]_i$ transients to $30.4 \pm 1.4\%$ while $200 \mu\text{mol l}^{-1} \text{Cd}^{2+}$ caused a drop to $2.5 \pm 0.2\%$. $200 \mu\text{mol l}^{-1} \text{Ni}^{2+}$ decreased the peak of the transients to $69.6 \pm 2.9\%$. Comparison of the blocking effects of divalent cations on Ca^{2+} currents and $[\text{Ca}^{2+}]_i$ transients supports further the conclusion that the depolarization-induced $[\text{Ca}^{2+}]_i$ changes are produced mainly by the activation of the HVA Ca^{2+} channels.

Key words: Isolated neurones — Voltage gated Ca^{2+} currents — Cytoplasmic $[\text{Ca}^{2+}]_i$ transients — Divalent Ca^{2+} channel blockers

Introduction

Neuronal functions are influenced by calcium ions in several ways. On depolarization of the nerve cells, for example, voltage-gated Ca^{2+} channels open allowing Ca^{2+} to enter and elevate cytoplasmic Ca^{2+} concentration ($[\text{Ca}^{2+}]_i$). In turn, the $[\text{Ca}^{2+}]_i$ transients produced can profoundly modify the membrane properties of the

neurones as well as their Ca^{2+} -dependent intracellular regulatory mechanisms. Beside these effects, the voltage-gated Ca^{2+} channels play important roles themselves in determining the excitatory processes developing on the surface membrane (see e.g., Kostyuk and Verkhratsky 1995).

There are data indicating that Ca^{2+} is involved in regulating the activity of the cochlear neurones, and certain cells in the dorsal part of the nucleus may even produce Ca^{2+} -dependent spikes (Hirsch and Oertel 1988). Patch-clamp studies on pyramidal neurones of the dorsal cochlear nucleus revealed that all known voltage-gated Ca^{2+} channel subtypes were present in these cells (Harasztosi et al. 1999; Molitor and Manis 1999). In these studies specific blockers of the so-called high-voltage activated (HVA) Ca^{2+} channels were applied. Using the same approach we showed that among these Ca^{2+} channel subtypes the N-type one was the most significant in producing depolarization-evoked $[\text{Ca}^{2+}]_i$ transients (Rusznák et al 2000).

In contrast to the HVA channels, low-voltage activated (LVA) or T-type Ca^{2+} channels do not have highly specific blockers. Some data indicate, however, that certain divalent cations show preferences when blocking the voltage-gated Ca^{2+} channels. Cd^{2+} , for example, is more effective in decreasing HVA currents while Ni^{2+} reduces LVA currents to a greater extent (for a review see e.g., Huguenard 1996).

To study the possible role of depolarization-activated Ca^{2+} channels in causing $[\text{Ca}^{2+}]_i$ elevations, experiments were carried out first to describe the influence of divalent Ca^{2+} channel blockers on Ca^{2+} currents, and then on the K^+ depolarization-activated $[\text{Ca}^{2+}]_i$ transients. Comparison of the blocking effects strengthened further the decisive role that the HVA Ca^{2+} channels play in producing depolarization-induced $[\text{Ca}^{2+}]_i$ transients of the pyramidal cells of the dorsal cochlear nucleus (DCN). Some of the results have been published in an abstract (Harasztosi et al 1998).

Materials and Methods

Cell isolation, chemicals, solutions

The basic steps of the isolation procedure were identical with those described by Harasztosi et al. (1999). After decapitating the 6–11-day-old rats, their brains were removed and incubated in a Na^+ -free artificial cerebrospinal fluid (-2°C ; aCSF, see below). The two cochlear nuclei were removed and their dorsal parts soaked for 40–55 minutes at 31°C in aCSF containing 0.03 mg/ml collagenase (type IA) and 0.12 mg/ml pronase (type XIV); the incubating solution was bubbled with 95% O_2 and 5% CO_2 throughout. After terminating the enzyme exposure by applying trypsin inhibitor (type I-S, 1 mg/ml), the brain pieces were mechanically triturated in HEPES-buffered aCSF.

The aCSF was made of (in $\text{mmol}\cdot\text{l}^{-1}$): NaCl 125; KCl 2.5; glucose 10; NaH_2PO_4 1.25; NaHCO_3 26; CaCl_2 2; MgCl_2 1; myo-inositol 3; ascorbic acid 0.5; Na-pyruvate

2 (all chemicals were purchased from Sigma, St. Louis, USA unless specified otherwise). In the Na^+ -free aCSF, sucrose ($250 \text{ mmol}\cdot\text{l}^{-1}$) substituted NaCl. The HEPES-buffered aCSF consisted of (in $\text{mmol}\cdot\text{l}^{-1}$): NaCl 135; KCl 3; glucose 10; HEPES 10; sucrose 45; CaCl_2 2; MgCl_2 1. To prepare solutions with elevated extracellular Ca^{2+} concentrations (5 or $10 \text{ mmol}\cdot\text{l}^{-1}$), CaCl_2 was added in appropriate amounts.

For patch-clamp measurements, the pipette solution contained (in $\text{mmol}\cdot\text{l}^{-1}$): N-methyl-D-glucamine 145 (titrated with HCl); HEPES 4; MgCl_2 4; EGTA 5; phosphocreatinine 12; MgATP 2; Na_3GTP (Type II-S) 0.5. No corrections were applied for junction potentials (2–3 mV; Doughty et al. 1998). To improve the conditions of Ca^{2+} current recording, the control bath solution was HEPES-buffered aCSF with added $1 \mu\text{mol}\cdot\text{l}^{-1}$ TTX, $1 \text{ mmol}\cdot\text{l}^{-1}$ CsCl, $2 \text{ mmol}\cdot\text{l}^{-1}$ 4-aminopyridine and $5 \text{ mmol}\cdot\text{l}^{-1}$ TEA-Cl in order to minimize contaminating currents. The cells were continuously perfused with this control solution using a gravity-driven micropfusion system, which allowed rapid solution exchange by switching between six available channels. Drugs were applied to the vicinity of the neurone under investigation using the same apparatus. CoCl_2 solution was freshly made *prior to* the experiments; CdCl_2 , NiCl_2 and MnCl_2 were diluted from deep-frozen stock-solutions.

For recording intracellular $[\text{Ca}^{2+}]$, membrane-permeant Fura-2-AM was applied (TEFLABS, Austin, TX, USA). The control bath solution was a HEPES-buffered aCSF in which $35 \text{ mmol}\cdot\text{l}^{-1}$ NaCl was replaced by sucrose (low- Na^+ aCSF). In the high- K^+ external solutions, appropriate amounts of the $1 \text{ mol}\cdot\text{l}^{-1}$ KCl stock were added and osmotically equivalent sucrose quantities were omitted. Preparation of solutions containing divalent Ca^{2+} channel blockers, continuous perfusion of the cells as well as quick solution change were performed as described above.

Recording and analysis of the Ca^{2+} currents

Recording of the Ca^{2+} currents was performed using the whole-cell configuration of the patch-clamp technique (Hamill et al. 1981). After dissociation, the neurones were allowed to settle for 30 minutes *prior to* the current measurements (carried out at room temperature, 18–22°C). The isolated cells were visualised by an inverted phase-contrast microscope (Diaphot 300, Nikon, Japan). Pyramidal cells were identified on the basis of their triangular or elongated bodies and the presence of multiple processes (Harasztosi et al. 1999). Thick-walled borosilicate glass tubes (BioLogic Science Products GmbH, Germany) were used to fabricate patch-clamp pipettes having resistances of 1.5–3 M Ω when filled with the appropriate pipette solution (see above). The patch-clamp set-up contained an Axopatch 200 A amplifier connected to a TL-1 interface (Axon Instruments, USA). Data acquisition and analysis were performed with the pClamp 6.0 software (Axon Instruments, USA). Digitisation rate was 5 kHz, filtering of the current traces was done at 2 kHz (using a 4-pole Bessel filter). Capacitive currents were compensated electronically, while the leak currents were subtracted as values linearly extrapolated from signals ac-

companying small de- or hyperpolarizing pulses (applied from a holding potential of -75 mV). Series resistance ($2\text{--}15$ M Ω) was compensated by at least 40%.

Intracellular $[Ca^{2+}]$ measurements

To promote their longer survival, the freshly dissociated neurones were kept for 3–4 hours in a Dulbecco's modified Eagle medium (DMEM) containing 10% horse serum (5% CO₂ atmosphere, 37°C). In the last 30 minutes of the incubation $3 \mu\text{mol}\cdot\text{l}^{-1}$ Fura-2-AM was added to the DMEM and the cells were subsequently washed with low-Na⁺ aCFS at room temperature for at least 30 minutes.

The fluorimetric measurements were performed in a Deltascan-1 system (Photon Technology International, New Brunswick, USA) at room temperature. Pyramidal cells were alternately exposed to excitation light beams of 340 and 380 nm wavelengths. Light emission was measured at 510 nm using a digitisation rate of 50 Hz. The Ca²⁺-related emission intensities were determined by subtracting the background fluorescence values and the 340/380 ratios were calculated point to point (OSCAR software, Photon Technology International, New Brunswick, USA). The ratio curves were digitally filtered, and then converted to $[Ca^{2+}]$ values using the usual formula with parameters (R_{min} , R_{max} , apparent K_D) obtained in *in vitro* calibrations.

Statistical analysis

Results are given as mean \pm S.E.M. throughout. Statistical analysis was performed by Student's *t*-test. The level of significance was taken as $p < 0.05$.

Results

Identification of the Ca^{2+} currents

As our aim was to study the role of voltage-gated Ca²⁺ channels of the pyramidal cells, first experiments were carried out to identify Ca²⁺ currents by applying suitable ramp protocols. Earlier this method proved to be especially useful for testing the effects of specific HVA channel blockers in a fast but reliable way (Harasztosi et al. 1999). Fig. 1A gives the details of such a protocol. The cell was held at -75 mV, then a hyperpolarizing step of 250 ms to -120 mV was applied (to remove any voltage-dependent inactivation of the currents). Following this the membrane potential was changed linearly from -120 mV to $+30$ mV in 200 ms, and then set back to the -75 mV holding value (i.e. the rate of the membrane potential change during the ramp was 0.75 mV/ms). The current-voltage relationships shown in the figure were obtained from the current signals accompanying the ramps.

Although our pipette and bath solutions were composed to optimize the conditions for selective examination of the Ca²⁺ channel activity, we also confirmed the identity of the charge carriers by increasing the extracellular Ca²⁺ concentration from the control $2 \text{ mmol}\cdot\text{l}^{-1}$ to 5 ($n = 3$) and 10 $\text{mmol}\cdot\text{l}^{-1}$ ($n = 4$; Fig. 1A). The results were the same in all the neurones tested: the control current-voltage relationship showed two maxima, one around -55 mV and the other at about -15 mV

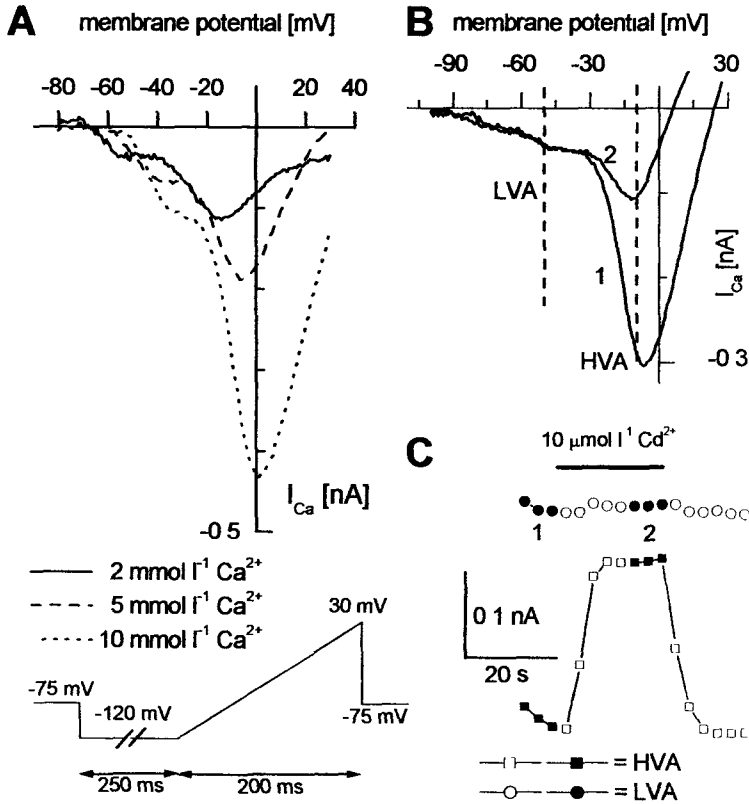


Figure 1. Effects of divalent cations on the LVA and HVA Ca^{2+} currents. **A.** Effects of changing extracellular Ca^{2+} concentration on Ca^{2+} currents. Current traces accompanying linear ramps were recorded (for pulse protocol see the inset). Current-voltage relationships were derived from the recorded current traces and displayed in the figure, first in control solution (2 mmol l^{-1} Ca^{2+} , continuous line), then in the presence of 5 mmol l^{-1} (broken line) and then 10 mmol l^{-1} external $[\text{Ca}^{2+}]$ (dotted line). **B.** Current-voltage relations derived from current traces accompanying 200 ms linear ramps from a -100 mV prepulse (250 ms, holding potential -75 mV) to $+30$ mV in control bath solution (trace 1) and in the presence of $10 \mu\text{mol l}^{-1}$ Cd^{2+} (trace 2). The amplitudes of the LVA and HVA currents were determined at -50 mV and -10 mV, respectively (denoted by vertical broken lines in the panel). The shift of the reversal potential towards more negative voltages following Cd^{2+} treatment indicates the presence of contaminating (possibly K^{+}) conductance(s). **C.** Time course of the same experiment as in panel B. The symbols give the LVA (circles) and HVA (squares) current amplitudes during the consecutive ramps (repeated in every 3 s). Filled symbols mark those ramps which were averaged (three in each case) and shown in panel B (the same numbers are used for identification). Thick horizontal bar indicates the application of the channel blocker.

indicating the presence of at least two inward current components with different voltage dependencies. These components reflected the contributions of both LVA and HVA Ca^{2+} channels to the recorded currents (Carbone and Lux 1984). Based on earlier findings in the rest of the experiments the current measured at -50 mV was considered as LVA current while that obtained at -10 mV was used to assess the contribution of the HVA components to the total Ca^{2+} current (Harasztosi et al. 1999).

Fig. 1A also demonstrates that the increased extracellular Ca^{2+} concentration resulted in higher amplitudes of both LVA and HVA components as well as in a shift of the activation threshold and both maxima of the current to more depolarized levels. The former observation can be explained by the increased electrochemical gradient for Ca^{2+} while the latter findings are due to the surface charge effect provided by the increased extracellular divalent cation concentration (Fox et al. 1987).

Effects of divalent cations on voltage-gated Ca^{2+} currents

In order to gain information about the pharmacological properties of the Ca^{2+} current components, effects of various well-known inorganic Ca^{2+} channel blockers were tested. Fig. 1B demonstrates how the application of $10 \mu\text{mol}\cdot\text{l}^{-1}$ Cd^{2+} modified the Ca^{2+} currents of a pyramidal cell. The current-voltage relationships presented are the averages of those derived from three consecutive current traces in control solution (trace 1) and in the presence of this low Cd^{2+} concentration (trace 2). In accordance with previous observations on other cell types (Fox et al. 1987; Huang 1989; Scott et al. 1991), in this concentration the Cd^{2+} powerfully inhibited the HVA component (to $26.6 \pm 2.5\%$ of the control; $n = 7$) while the T-type current was much less reduced (to $87.8 \pm 2.1\%$; $n = 7$; panel A of Fig. 3).

When the Cd^{2+} was applied at a concentration of $200 \mu\text{mol}\cdot\text{l}^{-1}$, both Ca^{2+} current components were strongly inhibited and the selectivity described above was much less obvious. As Fig. 3A indicates, the LVA current decreased to $32.4 \pm 2.7\%$ of the control ($n = 11$) and the HVA current to $11.7 \pm 2.1\%$ ($n = 12$). When the cells were subsequently perfused with a Cd^{2+} -free extracellular solution now containing $2 \text{mmol}\cdot\text{l}^{-1}$ Co^{2+} (not shown) inhibition of the LVA component became more pronounced ($11.1 \pm 1.7\%$ of the control; $n = 8$). The HVA current however was blocked to a smaller extent by the Co^{2+} ($28.9 \pm 5.4\%$ of the control; $n = 11$) than previously in the presence of $200 \mu\text{mol}\cdot\text{l}^{-1}$ Cd^{2+} .

In contrast to Cd^{2+} , Ni^{2+} blocks the T-type current more effectively than the HVA components (Fox et al. 1987; Huang 1989; Scott et al. 1991). Our findings indicated that the LVA current indeed proved to be somewhat more sensitive to $200 \mu\text{mol}\cdot\text{l}^{-1}$ Ni^{2+} (Fig. 3A): a decrease to $77.6 \pm 5.4\%$ of the control ($n = 5$) could be observed in the case of the LVA component while the HVA current was reduced to $86.9 \pm 2.6\%$ ($n = 7$).

We attempted the inhibition of the Ca^{2+} currents by the application of Mn^{2+} ($10 \text{mmol}\cdot\text{l}^{-1}$), too (not shown). The LVA current could be blocked very effectively

(decrease to $6.6 \pm 2.2\%$ of the control; $n = 3$) while the HVA current was inhibited to a smaller extent (to $28.4 \pm 8.1\%$; $n = 4$).

Effects of divalent Ca^{2+} channel blockers on $[\text{Ca}^{2+}]_i$ transients

It was described earlier that under the present experimental conditions the intracellular stores of the pyramidal cells usually contain only small amounts of Ca^{2+} at rest (Rusznák et al. 2000). The depolarization-induced $[\text{Ca}^{2+}]_i$ transients evoked consequently had to be based mainly on the entry of Ca^{2+} from the extracellular space. It was also shown in the same cell type that the activation of N-type channels played the most important role in producing the $[\text{Ca}^{2+}]_i$ transients. Lacking a specific blocker, however, there were no efforts to approximate pharmacologically the role of the LVA channels in influencing $[\text{Ca}^{2+}]_i$ elevations. As the experiments described above suggested that divalent cations showed some preferences when blocking LVA and HVA channels, we attempted to characterize the relative significance of the various voltage-gated Ca^{2+} channels in the genesis of the $[\text{Ca}^{2+}]_i$ transients on depolarizations by using some of these cations. Fig. 2 shows examples of these experiments in which effects of two divalent cations were tested.

Following the control transient, the neurone in panel A was incubated with $10 \mu\text{mol} \cdot \text{l}^{-1}$ Cd^{2+} then with $200 \mu\text{mol} \cdot \text{l}^{-1}$ Ni^{2+} and $[\text{Ca}^{2+}]_i$ transients were evoked during the incubation periods as well. Panel B presents another neurone where the

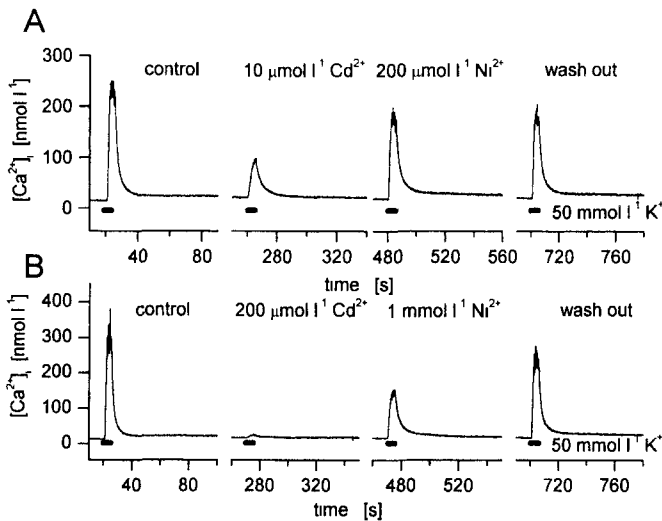


Figure 2. Effects of Cd^{2+} and Ni^{2+} on the depolarization-induced $[\text{Ca}^{2+}]_i$ transients. **A.** $10 \mu\text{mol l}^{-1}$ Cd^{2+} and $200 \mu\text{mol l}^{-1}$ Ni^{2+} were applied in the course of the experiment. 50mmol l^{-1} extracellular K^+ treatments evoked $[\text{Ca}^{2+}]_i$ transients before (control), during and after (wash out) the divalent cation treatments. Only those segments of the records are displayed where the $[\text{Ca}^{2+}]_i$ transients can be observed. **B.** Experiment executed similarly as above except that both the Cd^{2+} and the Ni^{2+} were added in higher concentrations ($200 \mu\text{mol l}^{-1}$ and 1mmol l^{-1} , respectively).

same protocol was applied but the concentrations of the blockers were different.

Panel B of Fig. 3 summarises the experiments carried out in a similar way. The Cd^{2+} was rather effective in blocking the depolarization-induced $[\text{Ca}^{2+}]_i$ transients, as in a concentration of $10 \mu\text{mol}\cdot\text{l}^{-1}$ it decreased their amplitudes to $30.4 \pm 1.4\%$ of the control ($n = 5$). Moreover, $200 \mu\text{mol}\cdot\text{l}^{-1}$ Cd^{2+} almost completely abolished the increase in intracellular $[\text{Ca}^{2+}]_i$ (a decrease to $2.5 \pm 0.2\%$ of the control; $n = 4$). On the other hand, Ni^{2+} , even at a relatively high ($200 \mu\text{mol}\cdot\text{l}^{-1}$) concentration, reduced the transients only to $69.6 \pm 2.9\%$ of the control ($n = 4$).

Discussion

The experiments of the present work yielded further support to the conclusion that although the pyramidal neurones isolated from the rat DCN possess both LVA and HVA Ca^{2+} channels in their surface membrane, the genesis of the depolarization-evoked $[\text{Ca}^{2+}]_i$ transients is based decisively on the activation of the HVA currents.

Advantages and difficulties of the applied experimental approach

As our aim was to explore the role of both LVA and HVA Ca^{2+} channels in modifying $[\text{Ca}^{2+}]_i$, we chose experimental conditions which might preserve the Ca^{2+} homeostasis of the isolated neurones as intact as possible. Patch clamping of the cells in the whole-cell configuration often causes a run-down of the Ca^{2+} currents. To prevent this phenomenon, instead of using long-lasting step protocols, we applied linear voltage ramps for activating Ca^{2+} currents. However, this approach obviously has certain disadvantages when interpreting data quantitatively.

Firstly, some of the T-type channels may inactivate during the ramp. We have shown earlier, however, that the voltage dependencies of both the LVA and the HVA currents were rather similar obtained either by step or by ramp protocols (Harasztosi et al. 1999).

Secondly, due to the overlap of the voltage dependencies, the choice of -10 and -50 mV for determining HVA and LVA current amplitude, respectively, may result in the overestimation of both components. This overestimation, in turn, may reduce the apparent selectivity of the LVA and HVA channel blockers.

Thirdly, $[\text{Ca}^{2+}]_i$ transients in the present study were evoked by increasing extracellular K^+ concentration. This manoeuvre is more suitable for long-lasting measurements, and applying K^+ depolarizations did not allow us as precise control of the membrane potential as voltage clamping of the neurones would. As we have not measured the membrane potential of the neurones, we could only estimate the magnitude of the K^+ depolarizations.

LVA and HVA Ca^{2+} currents in isolated DCN pyramidal neurones

Nerve cells possess a rather broad variety of voltage-gated Ca^{2+} channels. Although these channels show somewhat different kinetic properties and dependencies on the membrane potential, these features allow only the separation of the T-type (or LVA) current from the HVA ones by applying conditioning prepulses under voltage-clamp

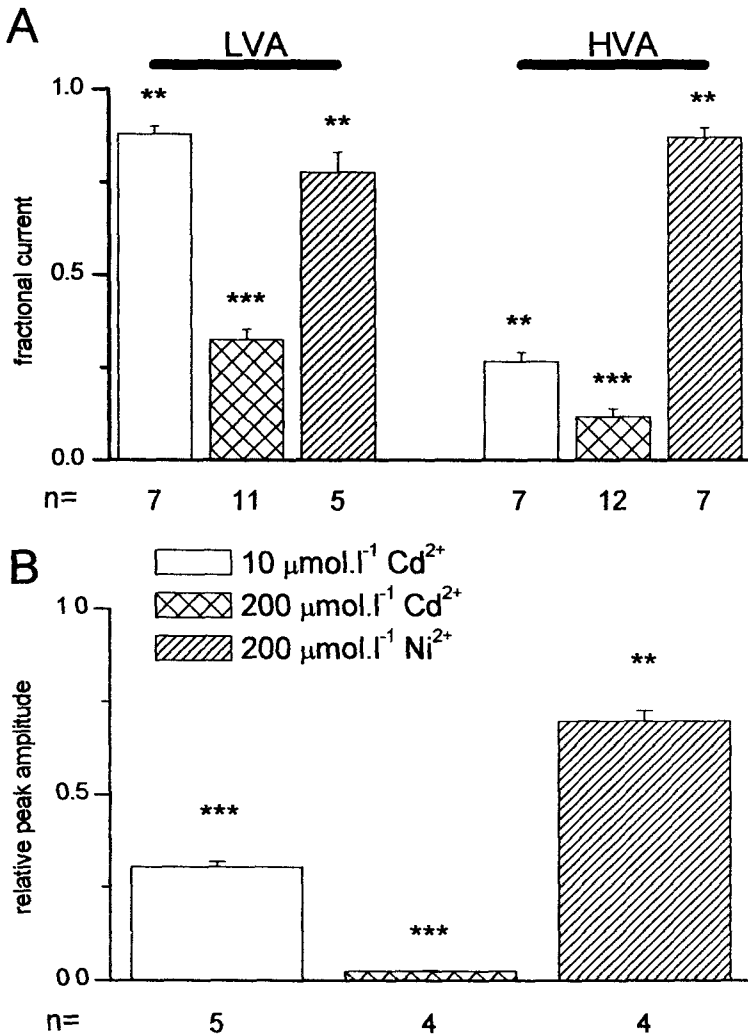


Figure 3. Synopsis of the effects of Cd²⁺ and Ni²⁺ on voltage-gated Ca²⁺ currents and K⁺ depolarization-evoked [Ca²⁺]_i transients. All measurements were carried out similarly to those illustrated in Figs 1 and 2. **A.** Fractional current means the size of the current measured in the presence of the divalent cations expressed as the fraction of the current of the same cell under control conditions. **B.** To calculate relative peak amplitudes the maximum values of the [Ca²⁺]_i transients seen in the presence of the blockers were measured and referred to the control peak value obtained in the same cell. To characterize the blocking effectiveness statistically, the absolute control values and those obtained during divalent cation treatments were compared. Error bars give S E M, the stars indicate the level of the statistical significance (** = 0.01 and *** = 0.001).

conditions. Using this method we studied earlier the presence and pharmacological modulation of HVA Ca^{2+} channels in isolated DCN pyramidal cells (Harasztosi et al. 1999).

Another possible way of testing the role of channel subtypes may be the application of specific blockers. Indeed, numerous voltage-gated Ca^{2+} channels have specific blockers but this is not the case with the LVA current. Considering these possibilities we decided to use the divalent cation blockers of the Ca^{2+} channels which are not highly specific but are reported to influence LVA and HVA channels differently (for reviews see e.g., Scott et al. 1991; Huguenard 1996). In isolated chicken DRG neurones, for example, $50 \mu\text{mol}\cdot\text{l}^{-1}$ Cd^{2+} almost completely suppressed the HVA currents but decreased the LVA component only by 45% (Fox et al. 1987; Tsien et al. 1988). $100 \mu\text{mol}\cdot\text{l}^{-1}$ Ni^{2+} was reported, however, to minimally influence the HVA currents and to block LVA current by 90%. Similar preferences were described in dissociated rat dorsal horn neurones (Huang 1989) where $100 \mu\text{mol}\cdot\text{l}^{-1}$ Cd^{2+} completely blocked the Ca^{2+} current at +20 mV but only by 30% at -30 mV. $1 \text{ mmol}\cdot\text{l}^{-1}$ Ni^{2+} , on the other hand, more effectively decreased the Ca^{2+} currents at -30 mV (by 90%) than at +20 mV (by 60%).

When comparing data in the literature, a great variability in the experimental conditions, in the source of the studied neurones and in the concentration of the applied divalent cation blockers is encountered. Reviewing the effects of divalent cations on T-type channels, Huguenard (1996) suggested that the above mentioned preferences might not be present in central neurones. However, our data obtained in isolated DCN pyramidal cells (see part A of Fig. 3) are not completely in line with this suggestion, as $10 \mu\text{mol}\cdot\text{l}^{-1}$ Cd^{2+} clearly differentiated between HVA and LVA currents. Ni^{2+} , on the other hand, at a concentration of $200 \mu\text{mol}\cdot\text{l}^{-1}$ showed less obvious preference in blocking the T-type channels. On interpreting the effect of Ni^{2+} , it is important to note that this cation may block some subpopulations of the HVA currents, too (Magee and Johnston 1995).

It was a consistent finding in the present experiments that the cells investigated possessed both LVA and HVA Ca^{2+} currents, although the magnitude of the LVA (T-type) current was variable (Harasztosi et al. 1999). There are data indicating that the different Ca^{2+} channel subtypes have uneven distribution in the surface membrane of different neurones. In hippocampal cells the soma membrane contains mainly L- and N-type channels while the T- and R-type channels are present in higher densities in the apical dendrites (Christie et al. 1995; Magee and Johnston 1995). If the distribution of the voltage-gated Ca^{2+} channels is similarly uneven in the DCN pyramidal cells, a variable loss of the dendrites and, consequently, the T-type channels may explain both the variable size of the LVA current and the small selectivity in the blocking effect of Ni^{2+} .

Contribution of the major Ca^{2+} channel subtypes to $[\text{Ca}^{2+}]_i$ transients

Using specific blockers to evaluate the relative importance of the members of HVA Ca^{2+} channel family in the development of depolarization-induced $[\text{Ca}^{2+}]_i$ elevations we came to the conclusion that although all the known subtypes were involved,

quantitatively the most significant contribution was provided by the N-type channels (Rusznák et al. 2000). As among the HVA Ca^{2+} channels some characteristics of the N-type ones resemble most of those found in the case of the T-type channels (tendency to inactivate, activation threshold at relatively negative membrane potentials, see e.g. Fox et al. 1987), it was worth studying further the roles of LVA and HVA currents in eliciting $[\text{Ca}^{2+}]_i$ transients by comparing the effects of divalent Ca^{2+} channel blockers on the Ca^{2+} currents and $[\text{Ca}^{2+}]_i$ transients. This comparison revealed that the extent of the decrease of the transients caused by Cd^{2+} was closer to the percentage block of the HVA currents and was more pronounced than the decrease of the LVA currents. Ni^{2+} , on the other hand, decreased the amplitude of the $[\text{Ca}^{2+}]_i$ transients to a greater extent than it blocked either the HVA or the LVA currents.

The above findings are in accordance with the related data in the literature. In rat isolated DRG neurones, for example, $50 \mu\text{mol}\cdot\text{l}^{-1}$ Cd^{2+} decreased the depolarization-induced $[\text{Ca}^{2+}]_i$ transients by 76% while Ni^{2+} at the same concentration caused a block of 25% (Leybaert et al. 1993). In hippocampal pyramidal neurones $200 \mu\text{mol}\cdot\text{l}^{-1}$ Cd^{2+} more effectively blocked the $[\text{Ca}^{2+}]_i$ transients in the soma than in the dendrites. The Ni^{2+} ($100 \mu\text{mol}\cdot\text{l}^{-1}$) was less effective in general but preferentially decreased the transients in the dendrites (Christie et al. 1995). These differences could be readily explained by the uneven distribution of the voltage-gated Ca^{2+} channel subtypes. On working with cerebellar granule cells in slice preparations Kirischuk et al. (1996) showed that $50 \mu\text{mol}\cdot\text{l}^{-1}$ Ni^{2+} blocked the $[\text{Ca}^{2+}]_i$ transients evoked by $20 \text{mmol}\cdot\text{l}^{-1}$ K^+ while those elicited by $50 \text{mmol}\cdot\text{l}^{-1}$ K^+ were not influenced. This difference might be due to the fact that $20 \text{mmol}\cdot\text{l}^{-1}$ K^+ caused less depolarization and in this voltage range the contribution of the T-type channels to the $[\text{Ca}^{2+}]_i$ transients was greater.

On the basis of our findings and the above cited data we conclude that the K^+ depolarization-induced $[\text{Ca}^{2+}]_i$ transients of the isolated DCN pyramidal neurones are mainly due to the activation of HVA channels. Little but significant blocking effects of Ni^{2+} on the transients indicate, however, that T-type channels may not be negligible in the determination of the peak value of the transients as these channels are activated at more negative membrane potentials, hence during the early phase of the depolarization-evoked $[\text{Ca}^{2+}]_i$ increases.

Acknowledgements. This work was supported by grants from the Wellcome Trust (Collaborative Research Initiative Grant, Great Britain), the Hungarian Science Foundation (OTKA T31824), the Ministry of Welfare (Hungary, ETT 49/2000) and the Ministry of Culture and Education (Hungary, FKFP 1289/1997). The authors are indebted to Mrs I Varga for technical assistance.

References

- Carbone E, Lux H D (1984) A low voltage-activated, fully inactivating Ca channel in vertebrate sensory neurones. *Nature* **310**, 501–503

- Christie B R , Eliot L S , Ito K I , Miyakawa H , Johnston D (1995) Different Ca^{2+} channels in soma and dendrites of hippocampal pyramidal neurons mediate spike-induced Ca^{2+} influx J Neurophysiol **73**, 2553—2557
- Doughty J M , Barnes-Davies M , Rusznák Z , Harasztosi Cs , Forsythe I D (1998) Contrasting Ca^{2+} channel subtypes at cell bodies and synaptic terminals of rat anteroventral cochlear bushy neurones J Physiol (London) **512**, 365—376
- Fox A P , Nowycky M C , Tsien R W (1987) Kinetic and pharmacological properties distinguishing three types of calcium currents in chick sensory neurones J Physiol (London) **394**, 149—172
- Hamill O P , Marty A , Neher E , Sakmann B , Sigworth F J (1981) Improved patch-clamp techniques for high-resolution current recording from cells and cell-free membrane patches Pflugers Arch **391**, 85—100
- Harasztosi Cs , Rusznák Z , Szűcs G (1998) Contrasting high and low voltage-activated Ca^{2+} currents of the pyramidal neurones of the rat dorsal cochlear nucleus Eur J Neurosci **10**, 72
- Harasztosi Cs , Forsythe I D , Szűcs G , Stanfield P R , Rusznák Z (1999) Possible modulatory role of voltage-activated Ca^{2+} currents determining the membrane properties of isolated pyramidal neurones of the rat dorsal cochlear nucleus Brain Res **839**, 109—119
- Hirsch J A , Oertel D (1988) Intrinsic properties of neurones in the dorsal cochlear nucleus of mice, *in vitro* J Physiol (London) **396**, 535—548
- Huang L Y (1989) Calcium channels in isolated rat dorsal horn neurones, including labelled spinothalamic and trigeminothalamic cells J Physiol (London) **411**, 161—177
- Huguenard J R (1996) Low-threshold calcium currents in central nervous system neurons Annu Rev Physiol **58**, 329—348
- Kirischuk S , Voitenko N , Kostyuk P , Verkhratsky A (1996) Calcium signalling in granule neurones studied in cerebellar slices Cell Calcium **19**, 59—71
- Kostyuk P , Verkhratsky A (1995) Calcium signalling in the nervous system John Wiley & Sons, Chichester, New York, Brisbane, Toronto, Singapore
- Leybaert L , De Ley G , De Hemptinne A (1993) Effects of flunarizine on induced calcium transients as measured in fura-2-loaded neurons of the rat dorsal root ganglion Naunyn-Schmiedeberg's Arch Pharmacol **348**, 269—274
- Magee J C , Johnston D (1995) Characterization of single voltage-gated Na^+ and Ca^{2+} channels in apical dendrites of rat CA1 pyramidal neurons J Physiol (London) **487**, 67—90
- Molitor S C , Manis P B (1999) Voltage-gated Ca^{2+} conductances in acutely isolated guinea pig dorsal cochlear nucleus neurons J Neurophysiol **81**, 985—998
- Rusznák Z , Harasztosi Cs , Stanfield P R , Kovács L , Szűcs G (2000) Potassium-depolarization-induced cytoplasmic $[\text{Ca}^{2+}]$ transients in freshly dissociated pyramidal neurones of the rat dorsal cochlear nucleus Pflugers Arch **440**, 462—466
- Scott R D , Pearson H A , Dolphin A C (1991) Aspects of vertebrate neuronal voltage-activated calcium currents and their regulation Prog Neurobiol (Oxford) **26**, 485—520
- Tsien R W , Fox A P , Hirning L D , Madison D V , McCleskey E W , Miller R J , Nowycky M C (1988) Multiple types of neuronal calcium channels In Voltage-sensitive ion channels modulation by neurotransmitters and drugs (Eds G Biggio, P F Spano, G Toffano, G L Gessa), pp 1—10, Liviana Press, Padova